

## CVD Synthesis of Highly Graphitized Single-walled Carbon Nanotubes Using Nitrogen-pretreated Fe–Mo/MgO Catalyst

Gaurav Patil, Chetan Sarode, Rahul Patil, and Suresh Gokhale\*  
*Physical and Materials Chemistry Division, National Chemical Laboratory,  
Dr. Homi Bhabha Road, Pune 411008, India*

(Received May 29, 2012; CL-120461; E-mail: sp.gokhale@ncl.res.in)

Single-walled carbon nanotubes (SWNTs) with highly graphitized structure were synthesized by thermal chemical vapor deposition using an improved nitrogen-pretreated Fe–Mo/MgO catalyst. The effects of nitrogen pretreatment of Fe–Mo/MgO on the structure and properties of SWNTs were studied by TEM, Raman spectroscopy, and TGA. The investigations revealed that the nitrogen pretreatment of the catalyst promoted the growth of SWNTs. It also enhanced the structural features and thermal properties of SWNTs.

Since their discovery in 1991,<sup>1</sup> carbon nanotubes (CNTs) have been ruling the regime of nanoresearch for their remarkable structural, mechanical, thermal, electronic, and phonon properties.<sup>2</sup> It is because of these excellent properties, CNTs find their use in several applications such as high strength composites, catalytic reactions, hydrogen storage, field-emission displays, sensors, and so on.<sup>3</sup> Depending on the requirement of a particular application, CNTs are modified suitably by a postsynthesis functionalization or during the synthesis itself by controlling the process conditions. In the later case, CNTs are preferably synthesized by chemical vapor deposition (CVD). Among all methods of CNT synthesis, CVD is very amenable due to its flexibility in manipulating reaction parameters.<sup>4</sup> In a conventional CVD process, a transition-metal-based catalyst is activated in inert atmosphere to synthesize CNTs from a gaseous hydrocarbon. Several CVD methods have been reported for the synthesis of CNTs, including those at varying catalyst formulation and reaction parameters.<sup>5</sup> Chiral selective growth of single-walled CNTs (SWNTs) can be achieved during nucleation by changing the catalyst composition or structure and controlling the kinetic parameters.<sup>6</sup> CNTs doped with N<sub>2</sub> by introducing N<sub>2</sub> gas flow in the flow of reactant gases have also been studied for structural changes, mechanical applications, and catalytic reactions.<sup>7</sup> In this letter, we report the synthesis of highly graphitized SWNTs by employing improved nitrogen-pretreated Fe–Mo/MgO catalyst nanoparticles in a thermal CVD and study the effects of nitrogen pretreatment of the catalyst on the structure and properties of SWNTs. We demonstrate herein that simple nitrogen pretreatment can enhance the catalytic activity, which in turn can promote the CNT growth mechanism to form long length, highly graphitized CNTs.

The Fe–Mo/MgO catalyst containing 5 wt% of Fe–Mo in 9:1 ratio was prepared from Fe(NO<sub>3</sub>)<sub>3</sub>·9H<sub>2</sub>O (98+%, Sigma-Aldrich), (NH<sub>4</sub>)<sub>6</sub>Mo<sub>7</sub>O<sub>24</sub>·4H<sub>2</sub>O (99.98%, Sigma-Aldrich), and MgO nanopowder (Strem Chemicals). In a typical procedure, 0.5 g of MgO was taken in 10 mL of methanol and ultrasonicated for 20 min to obtain a suspension. In another beaker, 0.1628 g of Fe(NO<sub>3</sub>)<sub>3</sub>·9H<sub>2</sub>O and 0.0046 g of (NH<sub>4</sub>)<sub>6</sub>Mo<sub>7</sub>O<sub>24</sub>·4H<sub>2</sub>O were mixed in 10 mL of methanol and ultrasonicated for 20 min to

obtain a solution. This freshly prepared solution was added dropwise to the suspension of MgO under magnetic stirring at room temperature. The stirring was continued until methanol was completely removed from the mixture. The mixture was allowed to dry at room temperature and then ground to a fine powder. The resulting Fe–Mo/MgO catalyst powder was calcined at 650 °C for 7 h. For the synthesis of SWNTs, approximately 0.1 g of the Fe–Mo/MgO catalyst was spread on a quartz plate and placed in a tubular quartz reactor (Firstnano ET2000). The catalyst was heated in nitrogen gas at the flow rate of 1000 mL min<sup>-1</sup>, and the temperature of the reactor was raised to 950 °C in 14 min. The nitrogen gas flow was then replaced with a mixture of CH<sub>4</sub> and H<sub>2</sub> gases at the flow rate of 1000 and 200 mL min<sup>-1</sup> respectively. The thermal decomposition of CH<sub>4</sub> was carried out for 30 min<sup>8</sup>, and the reaction gases were replaced with nitrogen again for the cooling of SWNTs. For comparison, SWNTs were also grown on plain Fe–Mo/MgO with no nitrogen pretreatment. In this case, the heating and cooling steps were performed under argon atmosphere. The SWNTs so synthesized in two different ways were purified by a treatment with 7 M HNO<sub>3</sub>. The acid solution containing SWNTs was magnetically stirred for 12 h to remove the catalyst material. The SWNTs were then washed with deionized water and filtered using an 8 μm pore-size PTFE membrane (PALL Corporation). The samples of SWNTs were dried under a high wattage lamp.

For convenience, the samples have been labeled as (a) for the SWNTs on plain Fe–Mo/MgO with no nitrogen pretreatment and (b) for the SWNTs on nitrogen-pretreated Fe–Mo/MgO.<sup>9</sup> Both samples were characterized by TEM (FEI Tecnai F30), Raman spectroscopy (Horiba JY LabRAM HR800 spectrometer), and TGA (Seiko TG/DTA 32) to study the effects of nitrogen pretreatment of Fe–Mo/MgO on the structure and properties of SWNTs.

The TEM images in Figure 1 show the morphological changes in SWNTs due to N<sub>2</sub> pretreatment of the catalyst. The SWNTs in sample (b) are well-formed and isolated. They have better structural features, and the nanotubes possess no or very few defects. A representative nanotube is indicated by an arrow. The SWNTs in sample (a), on the other hand, are formed in bundles and have more defects on the surfaces of the nanotubes. The sample (b) contains longer nanotubes and, hence, high aspect ratio as compared to the SWNTs in sample (a). The average diameter of the nanotubes could be around 1.5 nm.

These observations can be supported by Raman analysis. Figure 2 shows the Raman spectra of sample (a) and sample (b). Both spectra show a strong peak around 1571 cm<sup>-1</sup> for G-band due to the in-plane oscillations of graphitic carbon and a weak peak around 1324 cm<sup>-1</sup> for D-band due to the structural disorder or defects in SWNTs. A peak at 2638 cm<sup>-1</sup> in sample (a) or 2593 cm<sup>-1</sup> in sample (b) is assigned to G'-band due to the

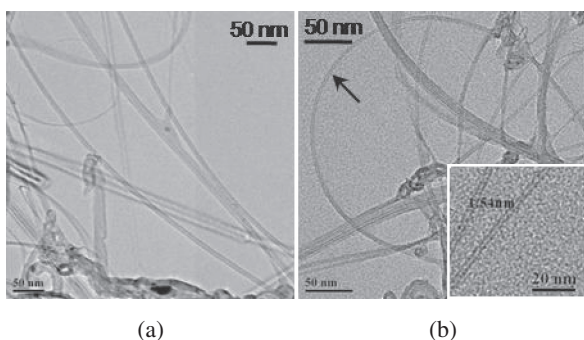


**Figure 1.** TEM images of SWNTs using plain Fe–Mo/MgO (a) and nitrogen-pretreated Fe–Mo/MgO (b). Inset shows a high-resolution image of two isolated SWNTs ( $d \approx 1.54$  nm).

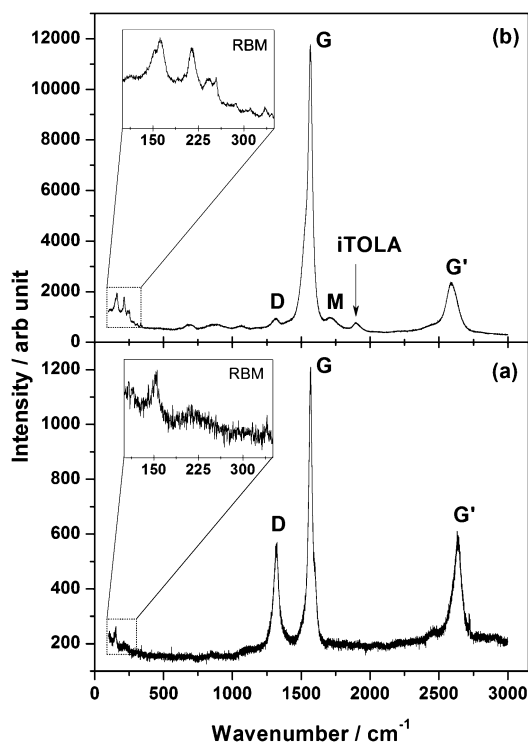


**Figure 2.** Raman spectra of CNTs using plain Fe–Mo/MgO (a) and nitrogen-pretreated Fe–Mo/MgO (b).

second-order Raman scattering relating to the D-band.<sup>8,10</sup> The peaks observed at 161 and 216  $\text{cm}^{-1}$  can be assigned to the C–C vibrations of SWNTs in radial breathing mode (RBM). The diameters of the nanotubes calculated using equation<sup>10</sup>  $\omega_{\text{RBM}} = 234/d + 10$  (where,  $\omega_{\text{RBM}}$  is the RBM wavenumber, and  $d$  is the diameter of SWNT) were found to be 1.5 and 1.1 nm. For typical SWNTs,  $d = 1.5 \pm 0.2$  nm has been reported.<sup>10</sup> In addition to these standard Raman features, the spectrum of sample (b) also shows weak double resonance features at 1729 and 1908  $\text{cm}^{-1}$  associated with the M-band and iTOLA second-order modes<sup>11</sup> respectively. M-band is attributed to the overtones of the out-of-plane graphitic carbon and iTOLA (the combination of iTOLA and LA modes) appears as a result of phonon dispersion of graphitic carbon.<sup>11</sup> This indicates that the SWNTs in sample (b) were isolated whereas the nanotubes in sample (a) were formed in

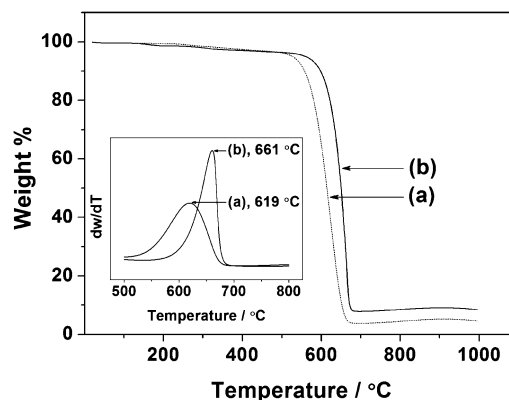


**Figure 3.** TGA graphs of SWNTs using plain Fe–Mo/MgO (a) and nitrogen-pretreated Fe–Mo/MgO (b). Inset shows the derivative curves for both samples.

bundles as these features are not seen in the spectrum of sample (a).

It is seen that the G-band for sample (b) is very intense as compared to that for sample (a). Therefore, it can be stated that the SWNTs in sample (b) were produced in large quantity and possessed higher degree of graphitization. The G-band around 1571  $\text{cm}^{-1}$  (for  $G^-$  feature, TO phonon) and its Lorentzian lineshape suggest the existence of semiconducting nanotubes.<sup>11</sup> The D-band for sample (b) is very marginal indicating the reduced defects in the structure and, thus, enhancement in the quality of SWNTs. The structural disorder or defects is directly proportional to  $I_D/I_G$ , the ratio of intensities of D-band to G-band. The  $I_D/I_G$  for sample (a) and sample (b) are 0.38 and 0.041 respectively. It has also been demonstrated that SWNTs show higher difference in the intensities of G-band and D-band.<sup>10</sup> Therefore, it can be stated that the SWNTs in sample (b) were highly graphitized and that the sample contained mostly SWNTs. The higher intensities of RBM peaks also support the fact that the sample (b) contained more SWNTs. The SWNTs in sample (a) were less graphitized, and the sample contained other crystalline forms of carbon causing structural defects in the nanotubes. The RBM peak intensities in the case of sample (a) are meager which suggest the presence of very few SWNTs.

The TGA graphs for sample (a) and sample (b) are shown in Figure 3. TGA graph shows the thermal degradation of various components present in a material, and its derivative determines the thermal stability of CNTs.<sup>12a</sup> As observed in the TGA graphs, the amount of amorphous carbon present in both samples was only 4%. The SWNTs in sample (b) started decomposing around 535  $^{\circ}\text{C}$  and decomposed completely at 690  $^{\circ}\text{C}$  whereas the nanotubes in sample (a) started decomposing around 496  $^{\circ}\text{C}$  and decomposed completely at 670  $^{\circ}\text{C}$ . Thus, the thermal stabilities of SWNTs were 535  $^{\circ}\text{C}$  for sample (b) and 496  $^{\circ}\text{C}$  for sample (a). From the derivative of TGA curves, the temperatures of half decomposition or the temperatures of maximum rate of decomposition were found to be 661  $^{\circ}\text{C}$  for sample (b) and 619  $^{\circ}\text{C}$  for sample (a). For vertically aligned SWNTs, the half decomposition temperature of 525  $^{\circ}\text{C}$  and thermal stability of 400  $^{\circ}\text{C}$  have been reported.<sup>12b</sup> This means that the SWNTs in sample (b) were more thermally stable than those in sample (a).

From all the above observations, it is inferred that the nitrogen pretreatment enhances the catalytic activity and

promotes the growth mechanism to yield longer SWNTs. The presence of nitrogen in the catalyst also seems to be responsible for improved graphitization of the nanotubes. In conclusion, we state that the nitrogen pretreatment of the catalyst produces long-length, highly graphitized SWNTs. We feel that the approach of this pretreatment can be further exploited for other catalysts.

The authors acknowledge the financial support by CSIR India under the Hydrogen Energy Network Program.

#### References and Notes

- 1 S. Iijima, *Nature* **1991**, *354*, 56.
- 2 a) M. S. Dresselhaus, G. Dresselhaus, J. C. Charlier, E. Hernández, *Philos. Trans. R. Soc., A* **2004**, *362*, 2065. b) J. Hone, M. C. Llaguno, N. M. Nemes, A. T. Johnson, J. E. Fischer, D. A. Walters, M. J. Casavant, J. Schmidt, R. E. Smalley, *Appl. Phys. Lett.* **2000**, *77*, 666. c) Phonon properties: Phonons play an important role as carriers in nanostructures. Thermal conductivity in CNTs is mainly due to phonons rather than electrons. Therefore, phonon scattering needs to be considered in thermal conduction processes, thermodynamic properties (e.g., heat capacity), electron-transport phenomena, and thermoelectricity.
- 3 a) V. N. Popov, *Mater. Sci. Eng., R* **2004**, *43*, 61. b) M. Endo, M. S. Strano, P. M. Ajayan, *Top. Appl. Phys.* **2008**, *111*, 13. c) J. M. Schnorr, T. M. Swager, *Chem. Mater.* **2011**, *23*, 646.
- 4 G. D. Nessim, *Nanoscale* **2010**, *2*, 1306.
- 5 a) M. Kumar, Y. Ando, *J. Nanosci. Nanotechnol.* **2010**, *10*, 3739. b) S. S. Mahajan, M. D. Bambole, S. P. Gokhale, A. B. Gaikwad, *Pramana* **2010**, *74*, 447.
- 6 R. Rao, D. Liptak, T. Cherukuri, B. I. Yakobson, B. Maruyama, *Nat. Mater.* **2012**, *11*, 213.
- 7 a) J. H. Yang, Y. J. Lee, Y. H. Kim, S. H. Moon, B. H. Ha, Y. S. Shin, S.-Y. Park, H. S. Kim, C. W. Yang, J.-B. Yoo, C.-Y. Park, *Jpn. J. Appl. Phys.* **2003**, *42*, 6713. b) G. F. Malgas, C. J. Arendse, N. P. Cele, F. R. Cummings, *J. Mater. Sci.* **2008**, *43*, 1020. c) Y. Ganesan, C. Peng, Y. Lu, L. Ci, A. Srivastava, P. M. Ajayan, J. Lou, *ACS Nano* **2010**, *4*, 7637. d) D. Yu, Q. Zhang, L. Dai, *J. Am. Chem. Soc.* **2010**, *132*, 15127. e) L. F. Mabena, S. S. Ray, S. D. Mhlanga, N. J. Coville, *Appl. Nanosci.* **2011**, *1*, 67.
- 8 S.-G. Kang, K.-K. Cho, K.-W. Kim, G.-B. Cho, *J. Alloys Compd.* **2008**, *449*, 269.
- 9 It was confirmed by EDX analysis that the N<sub>2</sub>-pretreated Fe–Mo/MgO catalyst contained approximately 4.14 wt % nitrogen. No nitrogen was present in the plain Fe–Mo/MgO catalyst.
- 10 S. Costa, E. Borowiak-Palen, M. Kruszyńska, A. Bachmatiuk, R. J. Kaleńczuk, *Mater. Sci.-Pol.* **2008**, *26*, 433.
- 11 M. S. Dresselhaus, G. Dresselhaus, R. Saito, A. Jorio, *Phys. Rep.* **2005**, *409*, 47.
- 12 a) L. S. K. Pang, J. D. Saxby, S. P. Chatfield, *J. Phys. Chem.* **1993**, *97*, 6941. b) H. M. Duong, E. Einarsson, J. Okawa, R. Xiang, S. Maruyama, *Jpn. J. Appl. Phys.* **2008**, *47*, 1994.